

## Impacts of adrenarcheal DHEA levels on spontaneous cortical activity during development

Samantha H. Penhale <sup>a</sup>, Giorgia Picci <sup>a</sup>, Lauren R. Ott <sup>a</sup>, Brittany K. Taylor <sup>a,b</sup>, Michaela R. Frenzel <sup>a</sup>, Jacob A. Eastman <sup>a</sup>, Yu-Ping Wang <sup>c</sup>, Vince D. Calhoun <sup>d</sup>, Julia M. Stephen <sup>e</sup>, Tony W. Wilson <sup>a,b,\*</sup>

<sup>a</sup> Institute for Human Neuroscience, Boys Town National Research Hospital, Boys Town, NE, USA

<sup>b</sup> Department of Pharmacology & Neuroscience, Creighton University, Omaha, NE, USA

<sup>c</sup> Department of Biomedical Engineering, Tulane University, New Orleans, LA, USA

<sup>d</sup> Tri-institutional Center for Translational Research in Neuroimaging and Data Science (TReNDS), Georgia State University, Georgia Institute of Technology, Emory University, Atlanta, GA, USA

<sup>e</sup> Mind Research Network, Albuquerque, NM, USA

### ARTICLE INFO

#### Keywords:

Magnetoencephalography (MEG)

Dehydroepiandrosterone

Resting-State

Adrenarche

Spontaneous cortical activity

### ABSTRACT

Dehydroepiandrosterone (DHEA) production is closely associated with the first pubertal hormonal event, adrenarche. Few studies have documented the relationships between DHEA and functional brain development, with even fewer examining the associations between DHEA and spontaneous cortical activity during the resting-state. Thus, whether DHEA levels are associated with the known developmental shifts in the brain's idling cortical rhythms remains poorly understood. Herein, we examined spontaneous cortical activity in 71 typically-developing youth (9–16 years; 32 male) using magnetoencephalography (MEG). MEG data were source imaged and the power within five canonical frequency bands (delta, theta, alpha, beta, gamma) was computed to identify spatially- and spectrally-specific effects of salivary DHEA and DHEA-by-sex interactions using vertex-wise ANCOVAs. Our results indicated robust increases in power with increasing DHEA within parieto-occipital cortices in all frequency bands except alpha, which decreased with increasing DHEA. In the delta band, DHEA and sex interacted within frontal and temporal cortices such that with increasing DHEA, males exhibited increasing power while females showed decreasing power. These data suggest that spontaneous cortical activity changes with endogenous DHEA levels during the transition from childhood to adolescence, particularly in sensory and attentional processing regions. Sexually-divergent trajectories were only observed in later-developing frontal cortical areas.

### 1. Introduction

Adolescence is ushered in by a cascade of hormonal events (i.e., puberty) and ends with the acquisition of adult social roles (Dahl, 2004). Pubertal development is characterized by two distinct endocrine events, adrenarche and gonadarche, both of which exert profound effects on the developing brain (for review, Goddings et al., 2019). The onset of puberty, adrenarche, is defined by the development of the adrenal cortex, which triggers a surge in androgens via the hypothalamic-pituitary-adrenal axis. It is thought that this process plays a key role in human brain development during the transition from childhood to adulthood (Byrne et al., 2017), but few studies have

systematically investigated its effects on the developing brain. More broadly, adrenarche instigates the formation of dehydroepiandrosterone (DHEA) around five to six years of age and throughout the adrenarcheal period, DHEA increases in both males and females, a finding that is highly consistent across studies (Whittle et al., 2015) and distinguishes it from its derivative pubertal hormones (i.e., testosterone and estradiol), which follow differential trajectories between sexes (Harden et al., 2014). DHEA continues to increase through adolescence and early adulthood, when it hits peak levels (Campbell, 2006; Rainey et al., 2002) and remains abundant throughout the lifespan (Corpéchot et al., 1981; Racchi et al., 2003). Although DHEA is a precursor to testosterone and estradiol, it is thought to additionally have a distinct role in puberty

\* Correspondence to: Boys Town National Research Hospital, 378 Bucher Circle, Boys Town, NE 68010, USA.

E-mail address: [tony.wilson@boystown.org](mailto:tony.wilson@boystown.org) (T.W. Wilson).

([Byrne et al., 2017](#); [Dorn and Chrousos, 1997](#); [Whittle et al., 2015](#)). Specifically, rises in DHEA are associated with pubic hair growth, body hair, and body odor, which represent the initial physical changes seen during puberty onset that occur as a function of adrenarche. Importantly, only a few studies have established neurodevelopmental links with normative changes in DHEA levels ([Byrne et al., 2017](#)), as existing work has largely focused on samples with premature adrenarche (e.g., [Klauser et al., 2015](#); [Whittle et al., 2015](#)) or the specific effects of testosterone and estradiol ([Goddings et al., 2019](#); [Wierenga et al., 2018](#)). To date, studies have shown that DHEA binds directly on androgen and estrogen receptors in the brain (e.g., [Prough et al., 2016](#)), suggesting there may be a neurological role of DHEA, however, the precise effects that DHEA has on the developing human brain are not well understood. Increases in DHEA during development are thought to occur in tandem with structural and functional changes in both cortical and subcortical regions ([Byrne et al., 2017](#)), but this is a relatively uncharted area of research. In large part, this is due to the standing literature focusing on the neurobiological effects of gonadarche, the second major endocrine event of puberty, which involves maturation of the hypothalamic-pituitary-gonadal axis.

Nevertheless, there is growing evidence for adrenal hormone effects on both anatomical and functional brain development. Specifically, a series of structural MRI studies have revealed mixed associations between DHEA concentrations and structural brain metrics in a regionally-specific manner during adrenarche ([Barendse et al., 2018](#); [Klauser et al., 2015](#); [Murray et al., 2016](#); [Nguyen et al., 2013, 2016](#)). For example, in several regions throughout the brain, [Nguyen et al. \(2013\)](#) reported a positive correlation between DHEA level and cortical gray matter thickness. Alternatively, white matter volume has been found to have a negative correlation with DHEA levels ([Klauser et al., 2015](#)). One study also found that children with higher levels of DHEA exhibited larger pituitary gland volumes ([Murray et al., 2016](#)). In terms of brain function, functional MRI (fMRI) studies have shown correspondence between DHEA levels and functional activation to emotional stimuli, primarily in frontal and temporal regions (e.g., cingulate, dorsal lateral prefrontal, and anterior temporal cortices; [Goddings et al., 2012](#); [Klapwijk et al., 2013](#); [Whittle et al., 2015](#)). However, these findings are also mixed, with reports of both positive and negative associations between DHEA and patterns of brain activation. These mixed results are likely due to methodological differences, including the use of different cognitive tasks and stimuli during fMRI. An alternative, complementary approach is to investigate how DHEA levels correspond to neural activity in the absence of task demands (i.e., resting-state). Prior work in adult participants has shown that exogenous administration of DHEA is related to decreases in amygdala-precuneus connectivity, suggesting modulatory effects of DHEA on brain function ([Sripada et al., 2013](#)). However, surprisingly, studies have yet to determine how DHEA varies with resting-state neural activity levels in a developmental sample. Importantly, resting-state fMRI approaches have shown great utility in the past two decades in uncovering age- and puberty-related changes in the functional organization of neural networks (e.g., [Fair et al., 2009](#); [Fareri et al., 2015](#)), but far less work has integrated hormonal measures and even fewer have investigated metrics like regional spectral power of neurophysiological signals to identify whether development is associated with changes in the strength of spontaneous cortical rhythms.

Building on the expansive fMRI resting-state literature, several recent studies have used magnetoencephalographic (MEG) approaches to address similar age- and hormone-related developmental questions ([Fung et al., 2020](#); [Ott et al., 2021](#)). Unlike other noninvasive neuroimaging techniques, MEG is able to capture regional spectral power, or spectrally specific spontaneous neural dynamics originating in the cortex due to its high spatial, spectral, and temporal precision. This is important in resting-state literature because it allows for observation of both where the amplitude of spontaneous cortical activity is changing and the precise rhythms involved (e.g., theta, alpha, etc.). For example, a previous study using MEG elucidated age- and sex-related effects in

spontaneous neural dynamics in adolescents across specific canonical frequency bands ([Ott et al., 2021](#)). In addition, several prior MEG studies have shown that task-related neural oscillatory dynamics are sensitive to critical indicators of development, including pubertal testosterone, and that this developmental sensitivity is modulated by sex ([Fung et al., 2020, 2021](#); [Killanin et al., 2020](#); [Taylor et al., 2021](#)).

Taken together, existing literature shows modulatory effects of pubertal hormones and sex on the development of cortical dynamics, but studies to date have yet to examine whether the development of spontaneous cortical rhythms are affected by the adrenal hormone, DHEA, which does not show the same degree of sexual-dimorphism compared to the gonadal hormones that have been more heavily studied (e.g., testosterone; [Goddings et al., 2019](#); [Harden et al., 2014](#); [Whittle et al., 2020](#)). Since there is a lack of clarity surrounding sex differences in DHEA during the pubertal period ([Orentreich et al., 1984](#); [Šulcová et al., 1997](#)), it is likely that any existing differences are subtle. Moreover, given that DHEA increases with age during adolescence, it is crucial to examine the effects of DHEA on neural function above and beyond age. Thus, the current study focused on the extent to which endogenous DHEA levels are related to spontaneous cortical dynamics in a developmental sample, while also examining potential interactive effects with sex. Because DHEA levels increase similarly in males and females (unlike gonadal hormones), we hypothesized that associations between DHEA and spontaneous cortical dynamics would be similar among both sexes, with minimal sexual divergence.

## 2. Methods

### 2.1. Participants

We enrolled 71 healthy children and adolescents (32 male;  $M_{age} = 13.07$  years,  $SD = 1.66$ , range = 9.99–16.99 years). Exclusionary criteria included any medical illness or medication known to affect CNS function, neurological or psychiatric disorders, history of head trauma, current substance abuse, and the standard exclusion criteria related to MEG acquisition (e.g., dental braces, metal implants, battery operated implants, and/or any type of ferromagnetic implanted material). All demographic data were reported by a parent or legal guardian as part of the intake process. Parents of the child participants signed informed consent forms, and child participants signed assent forms before proceeding with the study. The local Institutional Review Board reviewed and approved this study, and all protocols were in accordance with the Declaration of Helsinki.

### 2.2. Salivary DHEA collection and measurement

At least 2.0 mL of whole unstimulated saliva was collected from each participant. Specifically, children were asked to passively drool into an Oragene DISCOVER (OGR-500; [www.dnagenotek.com](#)) collection tube until liquid saliva (not bubbles) exceeded the fill line indicated on the tube. Participants were instructed to refrain from consuming any food, liquids, or chewing gum for at least an hour before providing the saliva sample, and generally completed the study in the afternoon. Prior to the release of the protease inhibitors for long-term storage, a single-channel pipette was used to extract 0.5 mL from the collection tube, which was immediately transferred into a labeled micro-centrifuge tube and placed in a –20 C freezer for storage. All samples were assayed with duplicate testing using a commercially-available assay kit for salivary DHEA ([Salimetrics](#); [www.salimetrics.com](#)) by the University of Nebraska Lincoln Salivary Biosciences Laboratory (<https://cb3.unl.edu/sbl/>). The assay kit had a sensitivity of 5 pg/mL, with a range of 10.2–1000 pg/mL. The intra- and inter-assay coefficients of variation were 7.95% and 10.17%, respectively. The averages of duplicate tests were used for analyses in the present study. A log transform was applied to DHEA measurements to account for skewness of the raw data (before transform: skewness = 2.82, kurtosis = 9.15; after transform: skewness =

0.32, kurtosis = -0.41).

### 2.3. MEG and MRI data acquisition

All MEG recordings took place in a one-layer magnetically-shielded room with active shielding engaged for environmental noise compensation. A 306-sensor MEGIN MEG system (Helsinki, Finland), equipped with 204 planar gradiometers and 102 magnetometers, was used to sample neuromagnetic responses continuously at 1 kHz with an acquisition bandwidth of 0.1 – 330 Hz. Participants were seated with their heads positioned within the sensor array and were instructed to rest with their eyes closed for six minutes. Throughout MEG data acquisition, participants were monitored by a real-time audio-video feed from inside the shielded room.

Structural T1-weighted images were acquired on a Siemens 3 T MRI scanner with a 32-channel head coil and a MPAGE sequence with one of the following parameters: TR = 2400 ms, TE = 1.94 ms, flip angle = 8°, FOV = 256 mm, slice thickness = 1 mm (no gap), base resolution = 256, 192 slices, voxel size = 1 mm<sup>3</sup>; or TR = 2300 ms, TE = 2.98 ms, flip angle = 9°, FOV = 256 mm, slice thickness = 1 mm (no gap), voxel size = 1 mm<sup>3</sup>. These structural images were only used for co-registration with the MEG functional data and visualization of the results, thus minor differences in MRI acquisition would not be expected to affect the MEG results.

### 2.4. Structural MRI processing and MEG-MRI coregistration

Participants' T1-weighted MRI data were segmented using the standard voxel-based morphometry pipeline in the computational anatomy toolbox (CAT12 v12.7; Gaser et al., 2022) within SPM12. T1 images underwent noise reduction using a spatially-adaptive non-local means denoising filter (Manjón et al., 2010) and a classical Markov Random Field approach (Rajapakse et al., 1997). An affine registration and a local intensity transformation were then applied to the bias corrected images. Finally, preprocessed images were segmented based on an adaptive maximum a posteriori technique (Ashburner and Friston, 2005) and a partial volume estimation with a simplified mixed model of a maximum of two tissue types (Tohka et al., 2004). Images were normalized to MNI template space and the resulting segmented files were then imported into Brainstorm for co-registration.

Prior to MEG acquisition, four coils were attached to the participant's head and localized, together with the three fiducial points and scalp surface, using a 3-D digitizer (Fastrak 3SF0002, Polhemus Navigator Sciences, Colchester, VT, USA). Once the participant was positioned for MEG recording, an electrical current with a unique frequency label (e.g., 322 Hz) was fed to each of the coils. This induced a measurable magnetic field and allowed each coil to be localized in reference to the sensors throughout the recording session. Since coil locations were also known in head coordinates, all MEG measurements could be transformed into a common coordinate system. With this coordinate system (including the scalp surface points), each participant's MEG data were co-registered with their structural MRI prior to source space analyses using Brainstorm.

### 2.5. MEG data pre-processing

Each MEG dataset was individually corrected for head motion and subjected to noise reduction using the signal space separation method with a temporal extension (tSSS; MaxFilter v2.2; correlation limit: 0.950; correlation window duration: 6 s; Taulu and Simola, 2006). MEG data processing was completed in Brainstorm (Tadel et al., 2019) and largely followed established analysis procedures (Niso et al., 2019). Briefly, a high pass filter of 0.3 Hz and a notch filter at 60 Hz and its harmonics were applied. Cardiac artifacts and eye movements were identified in the raw MEG data and removed using an adaptive signal-space projection (SSP) approach, which was subsequently

accounted for during source reconstruction (Ille et al., 2002; Uusitalo and Ilmoniemi, 1997). Data were then divided into four-second epochs and scanned for artifacts at the individual level. Briefly, in MEG, the raw signal amplitude is strongly affected by the distance between the brain and the MEG sensor array, as the magnetic field strength falls off sharply as the distance from the current source (i.e., brain) increases. To account for this source of variance across participants, as well as other sources of variance, we used an individualized threshold based on the signal distribution for both amplitude and gradient to reject artifacts. Specifically, epochs with amplitudes and/or gradients exceeding  $\pm 3$  SD of that participant's distribution of values were marked as bad and excluded from further analyses. The mean number of accepted epochs was 66.9 with a SD of 8.40 and a range of 54–104 epochs. The number of accepted epochs did not significantly vary as a function of age ( $r(65) = .12, p = .35$ ), sex ( $t(63) = -1.49, p = .14$ ), or DHEA ( $r(65) = .12, p = .36$ ).

### 2.6. MEG source imaging and frequency power maps

In accordance with prior literature (Niso et al., 2019), we computed minimum norm estimates normalized by a dynamic statistical parametric mapping (dSPM) algorithm for source imaging. To account for environmental noise, we utilized empty room recordings to compute a noise covariance matrix for source imaging (Baillet et al., 2001). The forward model was computed using an overlapping spheres head model (Huang et al., 1999). Finally, the imaging kernel of depth-weighted dSPM constrained to the individual cortical surface (Dale et al., 2000) was computed.

Using these source estimates, we then computed the power of cortical activity in canonical frequency bands: delta (2–4 Hz), theta (4–8 Hz), alpha (8–12 Hz), beta (15–30 Hz), and gamma (30–80 Hz). We used Welch's method for estimating power spectral densities (PSD; Welch, 1967) on each four-second epoch, with one second sliding Hamming windows overlapping at 50%. We then standardized the PSD values in each canonical frequency band to the total power across the frequency spectrum. For each participant, we averaged PSD maps across epochs to obtain one set of PSD maps per participant. Finally, we projected these maps onto the MNI ICBM152 brain template (Fonov et al., 2009) and applied a 3 mm FWHM smoothing kernel. These normalized source maps, showing the distribution of relative power in each frequency band, were used for further statistical analysis.

### 2.7. Statistical analyses

We analyzed the whole-brain PSD maps using ANCOVA models in SPM12 to identify spatially specific effects of DHEA and the interaction between DHEA and sex. Because DHEA is known to increase with age (Buck Louis et al., 2008), and because of recent work showing age-related changes in spontaneous cortical activity (Ott et al., 2021) we included age as a control variable in our statistical models. This allowed us to explore the unique effects of DHEA above and beyond the effects of age. Thus, for each frequency band, we ran an ANCOVA model with age as a continuous variable of no interest, DHEA as a continuous predictor, and sex as a categorical predictor, along with the respective DHEA-by-sex interaction term. To correct for multiple comparisons, we applied threshold free cluster enhancement (TFCE; Smith and Nichols, 2009) with a weighting factor of  $E = 0.6$ . Finally, TFCE maps were thresholded using the clusters that survived  $p < 0.05$  uncorrected with  $k > 100$ . TFCE values were averaged across individual clusters, separated by hemisphere. A cluster level family wise error (FWE) of 0.05 was applied to the remaining clusters to control for multiple comparisons and these data were used to display the corresponding effects.

### 3. Results

#### 3.1. Descriptive statistics

Of the 71 healthy youths who participated in the study, six had DHEA levels that were below the detection threshold. Thus, those participants were excluded from analysis. The results presented here include data from the remaining 65 participants (29 males,  $M_{age} = 13.22$  years,  $SD = 1.61$ ; range = 9.99 – 16.99 years). Demographic characteristics are detailed in Table 1.

#### 3.2. Spontaneous neural dynamics

Relative power was calculated across five canonical frequency bands: delta, theta, alpha, beta and gamma (Fig. 1). Patterns of power distribution varied between frequency bands, with delta, beta and gamma showing the highest relative power in anterior regions of the brain, theta having the highest relative power centrally, and relative alpha power being strongest in the posterior portion of the brain.

#### 3.3. DHEA and spontaneous neural dynamics

As mentioned previously, we examined the impact of DHEA on the developmental trajectory of spontaneous neural dynamics by computing a series of ANCOVA models. Specifically, we probed the main effect of DHEA and the interaction between DHEA and sex on spontaneous power. In all computed models, age was included as a variable of no interest due to its correlation with DHEA levels in the whole sample (Fig. 2). There were no significant differences between males and females in age or DHEA levels (Table 1). The data were modeled for each of the five frequency bands using TFCE and FWE 0.05 corrections. Clusters that were identified as significant are described in detail below.

#### 3.4. Main effects of DHEA

Models of spontaneous power revealed that increasing DHEA was associated with increases in spontaneous delta (Fig. 3; left:  $F(1, 60) = 10.975, k = 4427, p_{FWE} = 0.021$ ; right:  $F(1, 60) = 9.884, k = 3565, p_{FWE} = 0.022$ ) across occipital and parietal regions. Conversely, we found a main effect of DHEA in the alpha frequency band, such that relative power decreased with increasing DHEA. This effect was seen broadly across the parietal cortex, extending into the bilateral temporal cortices (right:  $F(1, 60) = 10.905, k = 5420, p_{FWE} = 0.013$ ; left:  $F(1, 60) = 10.463, k = 4793, p_{FWE} = 0.014$ ). Beta (right:  $F(1, 60) = 13.908, k = 1534, p_{FWE} = 0.023$ ; left:  $F(1, 60) = 12.898, k = 1270, p_{FWE} = 0.031$ ) and gamma power (right:  $F(1, 60) = 19.920, k = 2187, p_{FWE} = 0.008$ ; left:  $F(1, 60) = 14.502, k = 493, p_{FWE} = 0.017$ ) was observed to increase in relative power with increasing DHEA, concentrated in the occipital cortex. Table 2 provides the full ANCOVA results for each of the

canonical bands.

#### 3.5. DHEA-by-sex interaction

Interestingly, delta was the only frequency band that exhibited an interaction between DHEA and sex. Specifically, there was a significant DHEA-by-sex interaction in the right frontal, left frontal, and left temporal (Fig. 4; right frontal:  $F(1, 60) = 7.590, k = 153, p_{FWE} = 0.023$ ; left frontal:  $F(1, 60) = 8.106, k = 199, p_{FWE} = 0.024$ ; left temporal:  $F(1, 60) = 6.397, k = 195, p_{FWE} = 0.023$ ). In all clusters, females showed very gradual decreasing delta power with increasing DHEA levels, and males showed very gradual increasing delta power with increasing DHEA levels. Lastly, to ensure the greater number of females did not bias our analyses, we excluded seven female participants and reran all analyses using the remaining 29 participants per sex group. The results were virtually identical and thus all reported results include the full 65 participants described above in Section 3.1.

### 4. Discussion

In the present study, we examined the effect of DHEA on spontaneous cortical activity during the transition from childhood to adolescence in a large cohort of typically-developing youth. Specifically, we identified the relationship between DHEA levels and power within five canonical frequency bands (delta, theta, alpha, beta and gamma), above and beyond age. Further, we probed the interaction between DHEA and sex on these measures of spontaneous power. We found robust DHEA-specific effects across posterior brain regions in several frequency bands. Specifically, increasing DHEA levels were associated with increasing delta, beta and gamma power in bilateral parieto-occipital regions. Conversely, alpha power decreased with increasing DHEA levels across largely overlapping regions of the bilateral parieto-occipital cortices. Interestingly, delta was the only frequency band in which DHEA exhibited dissociable sex effects such that, with increasing DHEA levels, males showed gradually increasing delta power and females showed the opposite. This relationship was observed across three clusters spanning the bilateral frontal and left anterior temporal cortices.

DHEA is an adrenal steroid hormone that acts as a precursor to gonadal hormones like estradiol and testosterone (Goddings et al., 2019). Unlike its derivatives, which are known to vary between males and females (Goddings et al., 2019), one study showed that DHEA increases at a similar, linear rate for both males and females during the 8–14 year-old developmental period (Whittle et al., 2020), which is comparable to what we report in our sample of 9–16 year-olds. This could suggest that during pubertal development, sex-specific effects of DHEA on spontaneous cortical activity are less likely due to the lack of sexual divergence that is seen in DHEA levels between males and females. Indeed, in the current study, we observed similar levels of DHEA between males and females, and the majority of findings reported were main effects of DHEA, irrespective of sex.

DHEA was associated with the power of spontaneous activity in alpha, beta, and gamma, above and beyond age. Of note, these frequency bands have been implicated in attention and sensory processing (Wang et al., 2013). In fact, previous work has found alpha, beta, and gamma each to be important in mediating perception and attention, particularly in the parietal cortex (Misselhorn et al., 2019; Zaretskaya and Bartels, 2015). Specifically, during this developmental period, increases in theta activity have been reported during abstract reasoning (Taylor et al., 2020) and selective attention performance (Taylor et al., 2021), age-related changes in visual gamma activity have been seen during basic visual processing (Fung et al., 2021), alterations in alpha activity have been reported during verbal working memory processing (Embrey et al., 2019; Killanin et al., 2022), and beta and gamma oscillations have been found to change in relation to a developing sensorimotor system (Heinrichs-Graham et al., 2018; Trevarrow et al., 2019; Wilson et al., 2010). In the current study, beta and gamma activity

**Table 1**  
Demographic characteristics of the final sample.

	Male	Female	t/chi-square value	p-value
Mean Age (years)	13.53	12.97	.45	.66
Age Range (years)	9.99–16.99	10.61–16.34	–	–
Mean DHEA (ln(pg/mL))	3.40	3.49	.39	.70
DHEA Range (ln(pg/mL))	1.98–5.28	1.64–5.80	–	–
Race (White/Black or African American/Other/Unknown)	27/1/1/0	29/2/3/2	1.01	.60
Ethnicity (Not Hispanic or Latino/ Hispanic or Latino)	29/0	33/3	2.53	.11
Handedness (R/L/both)	28/0/1	35/1/0	2.05	.36

Note: Differences in age between males and females were assessed using an independent samples t-test; differences in race, ethnicity, and handedness were assessed using a chi-square test.

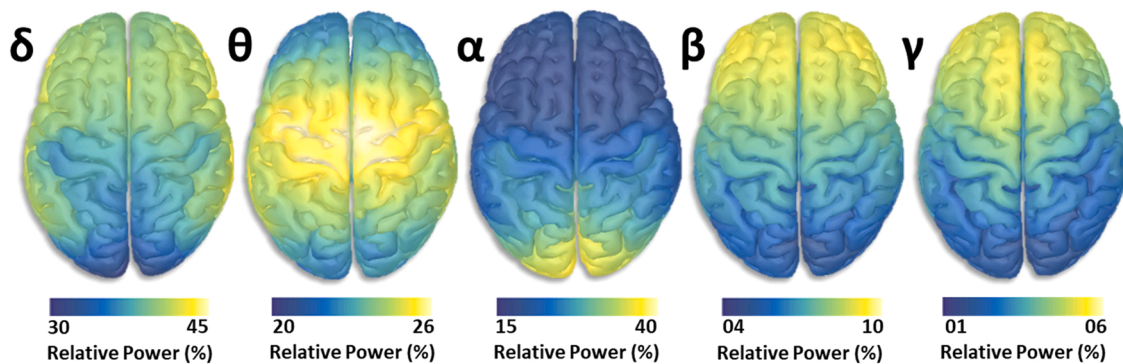


**Fig. 1.** Relative power in each frequency band: Template brains show grand averaged relative power maps, with color bars scaled to the minimum and maximum values of each map. Power distribution is shown for the five frequency bands. From left to right, these include delta, theta, alpha, beta, and gamma.

## DHEA Correlation with Age by Sex

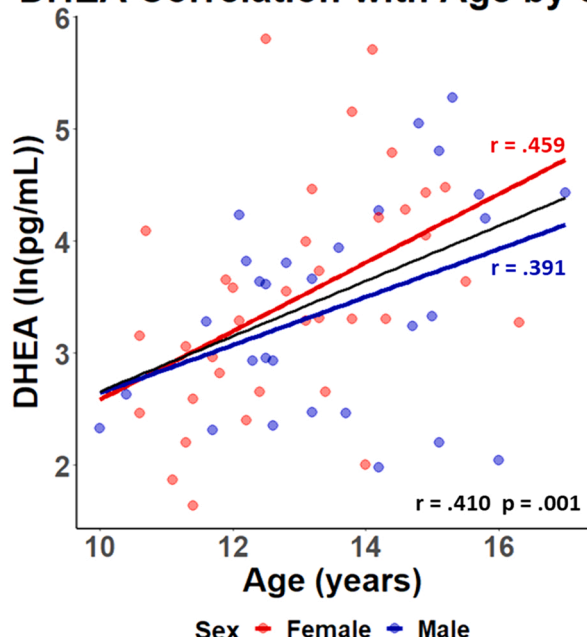


**Fig. 2.** Correlation between DHEA and Age: A scatter plot displays the correlation between DHEA and age for each sex. The natural log of DHEA is plotted on the y-axis and age is plotted on the x-axis, with individually plotted points representing each participant. Males ( $r = .391$ ) and females ( $r = .459$ ) are plotted separately to enhance clarity. An additional black trendline represents the entire sample ( $r = .410, p = .001$ ).

increased with increasing DHEA in posterior parietal and occipital regions of the brain, which are in line with roles in attention and early sensory processing. Thus, these relationships may reflect that these processing capabilities are fine-tuned behaviorally and neurally during this period of development (Morandini et al., 2021).

Conversely, our results revealed that alpha power decreased with increasing DHEA in parieto-occipito-temporal regions. In these brain regions, alpha has formerly been associated with cortical inhibition of visual sensory input (Heinrichs-Graham and Wilson, 2015; McDermott et al., 2017; Proskovec et al., 2016, 2018; Wiesman et al., 2017; Wilson et al., 2017). For example, several studies have reported alpha oscillations in the left parieto-occipito-temporal cortices during the encoding and maintenance phases of verbal working memory tasks. Presumably such activity reflects active encoding and rehearsal of the language-based visual stimuli, as well as attention processes (McDermott et al., 2017; Proskovec et al., 2016, 2018; Wiesman et al., 2017).

Similar findings have been observed in developmental populations such that these alpha responses appear to become stronger with increasing age during the development of working memory (Embry et al., 2019). Further, many of these same studies have shown robust alpha dynamics in parieto-occipital cortices during maintenance phase, when participants are actively rehearsing the stimuli presented during the encoding phase and suppressing incoming visual information that could act as interference (Heinrichs-Graham and Wilson, 2015). These alpha responses are thought to be largely distinct, as their time courses and direction (increase/decrease) are distinct. The findings in the current study, which link DHEA to shifts in alpha power in parieto-occipital regions, may allude to refinement of working and attention circuitry, but future studies using such paradigms are needed to verify such a relationship.

Of interest, delta was the only frequency band in which an interaction effect between DHEA and sex was uncovered in the frontal and temporal lobes. This is unsurprising, given that the frontal and temporal lobes are among the last to develop during adolescence, both in terms of structure and function (Bludau et al., 2014; Fuster, 2002; Gogtay et al., 2004; Romine and Reynolds, 2005; Tsujimoto et al., 2011). Further, delta power has been found to have strong developmental effects, particularly in frontal regions, and changes in delta power appear to continue throughout the lifespan (Gómez et al., 2013; Ott et al., 2021; Vlahou et al., 2014). Prevailing theoretical and empirical work on adolescent brain development suggests there are DHEA-related alterations to the frontal and temporal lobes, in particular (Goddings et al., 2012; Nguyen et al., 2013). However, these studies have not examined any sexually-dimorphic interactions associated with these alterations, which the present study more closely probed. For example, one previous fMRI study in only female adolescents revealed positive associations between DHEA levels and activity in the left anterior temporal cortex during an emotion processing task (Goddings et al., 2012). Together with the current study, this suggests that DHEA-specific effects in temporal regions are detected across neuroimaging modalities, and in both task-dependent and task-free designs. The current study further builds upon prior research by incorporating both males and females to help disentangle how adrenal hormones, above and beyond age, are associated with cortical activity. Given our inclusion of both sexes, we were able to identify differential trajectories in relation to sex, with males showing increases in delta with increasing DHEA while females show the opposite. Moreover, the present study included a wider swath of development compared to previous work, which included only 11–13-year-old youths and thus may not have been fully representative of the developmental course of adrenarche.

Further, our results build upon prior studies of DHEA in that they provide a link between production of adrenal hormones and changes in spontaneous cortical activity, filling the gap that currently exists in this area of research. The effects of DHEA unveiled in this study were all in regions spanning the parietal and occipital cortices, extending into

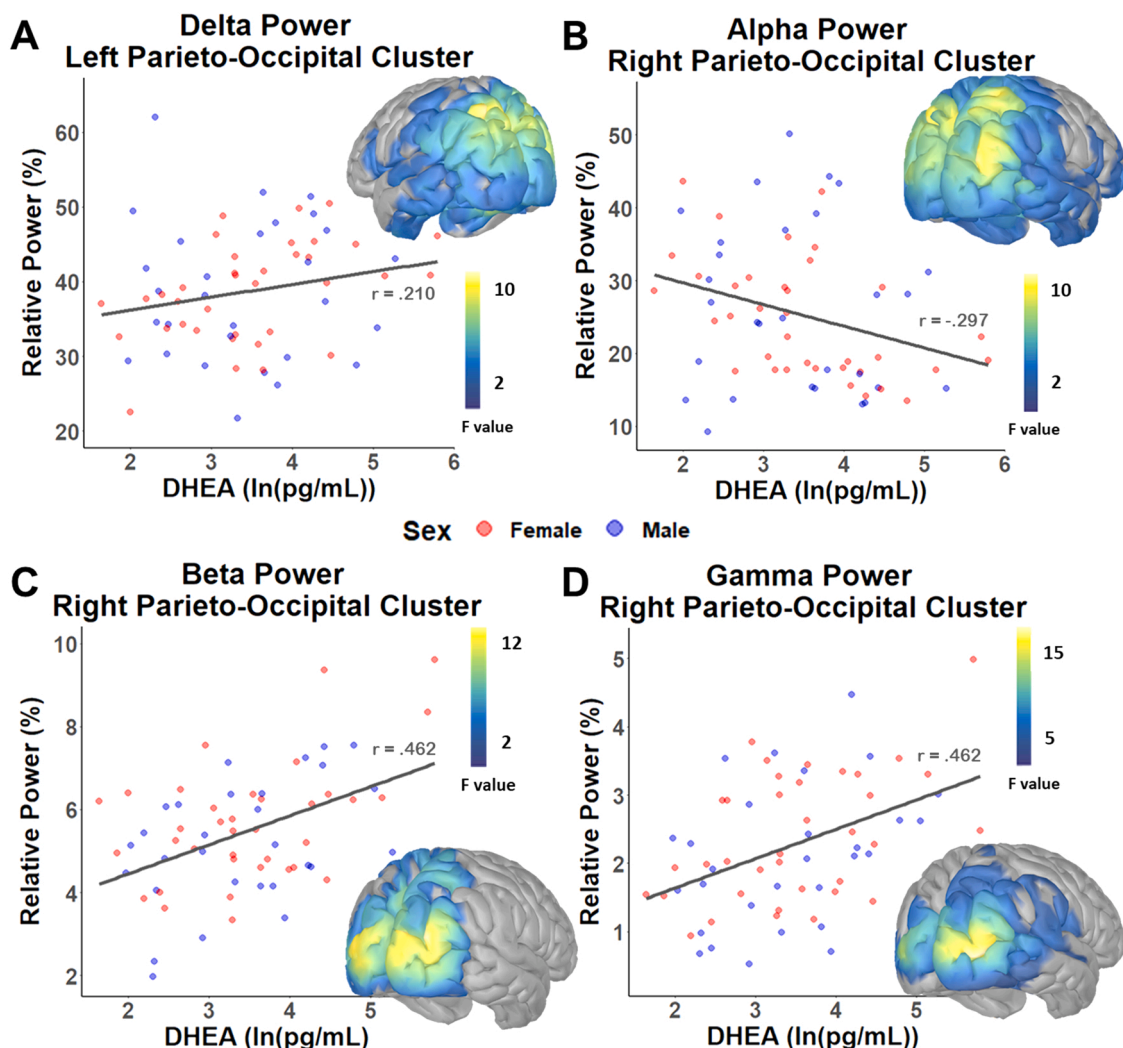


**Fig. 3.** Main Effect of DHEA: Scatter plots display the significant effect of DHEA on relative power. Relative power across the significant cluster denoted in the title is plotted for each participant on the y-axis and the natural log of DHEA is plotted on the x-axis. Trendlines are plotted on each graph to represent an increase or decrease in relative power with DHEA. Note that the scatterplots reflect the strongest cluster, but the effects were virtually identical across the other clusters (i.e., sub-peaks) per map. F-maps were thresholded using a TFCE mask at  $p < 0.05$  uncorrected with  $k > 100$ , as to only display significant effects, and are displayed with a color bar showing the scale of F values from weakest (blue) to strongest (yellow). Areas of the brain in gray are nonsignificant. DHEA has significant effects in posterior clusters in four frequency bands. Delta power increased in bilateral parietal clusters with increasing DHEA (A; left:  $r = .210$ ; right:  $r = .230$ ). Alpha power decreased in bilateral parieto-occipital clusters with increasing DHEA (B; left:  $r = -.287$ ; right:  $r = -.297$ ). Relative power increased in bilateral occipital regions in both beta (C; left:  $r = .463$ ; right:  $r = .462$ ) and gamma (D; left:  $r = .463$ ; right:  $r = .462$ ) frequency bands with increasing DHEA.

inferior temporal regions. This is consistent with structural MRI research showing vast developmental changes in brain structure are occurring throughout the transition from childhood to adolescence (Blakemore et al., 2010; Wierenga et al., 2014). Specifically, studies show that primary sensory areas, including the primary occipital and temporal cortices, reach peak volume and thickness first, closely followed by parietal regions (Blakemore et al., 2010; Shaw et al., 2008; Sowell et al., 2004; Wierenga et al., 2014). Additional research has suggested that adrenarche is closely tied with structural brain development (Barendse et al., 2018; Klauser et al., 2015; Nguyen et al., 2013). In fact, a prior study found DHEA levels to be related to cortical thickness and volume of both the left occipital pole and the right parietal lobe (Nguyen et al., 2016), similar regions to where our data displayed effects of DHEA on spontaneous cortical activity. Future work will need to build upon this by capturing adrenarche and gonadarche (i.e., sex-steroid hormone effects) processes longitudinally to elucidate how these processes unfold and alter cortical dynamics subserving the transition from adolescence into adulthood.

Despite a number of strengths, there remain several limitations of the

current study that must be noted. First, the secretion of DHEA is not restricted to the early-pubertal period; DHEA levels continue to rise into early adulthood as the adrenal glands gradually mature throughout adrenarche. From here, the hormone remains abundant in circulation throughout the lifespan. Throughout the course of the lifespan, DHEA is known to act through a number of mechanisms as well, such as binding sex steroid receptors, synergizing with sex steroid hormones, inhibiting GABAergic responses and potentiating NMDA-mediated signaling, and occurring through de novo synthesis within the CNS, which cannot be fully ruled out or controlled for in the current study (Mellon and Griffin, 2002). Relatedly, the onset of adrenarche is unique to each individual and the current study did not capture the onset of this process, per se, only interindividual variability. Thus, examining these processes in a younger sample would be beneficial to capturing the onset of adrenarche with the explicit aim of disentangling the production of adrenal hormones from the production of gonadal hormones. However, Whittle and colleagues (2020) found a linear increase in children ages 8–14, so it is likely we are capturing the majority of this linear increase across the current study. In order to fully ascertain which stages of puberty

**Table 2**  
Table of ANCOVA results.

Frequency/ Cluster	Effect	Cluster Size (voxels)	Peak Coordinates (MNI: x y z)	F-Value (from peak)	p- FWE Value
Delta RP	DHEA Main Effect	3565	32 – 68 29	9.884	0.022
Delta LP	DHEA Main Effect	4427	-10 – 56 30	10.975	0.021
Alpha RP	DHEA Main Effect	5420	36 – 79 23	10.905	0.013
Alpha LP	DHEA Main Effect	4793	-5 – 68 43	10.463	0.014
Beta RO	DHEA Main Effect	1534	34 – 89 25	13.908	0.023
Beta LO	DHEA Main Effect	1270	-29 – 98 19	12.898	0.031
Gamma RO	DHEA Main Effect	2187	38 – 92 6	19.92	0.008
Gamma LO	DHEA Main Effect	493	-26 – 102 13	14.502	0.017
Delta RF	DHEA x Sex Interaction Effect	153	19 61 – 7	7.59	0.023
Delta LF	DHEA x Sex Interaction Effect	199	-35 33 – 23	8.106	0.024
Delta LT	DHEA x Sex Interaction Effect	195	-60 5 – 33	6.397	0.023

Note: RP: Right Parietal; LP Left Parietal; RO: Right Occipital; LO: Left Occipital; RF: Right Frontal; LF: Left Frontal; LT: Left Temporal

participants are in, other measures of pubertal development will be necessary for subsequent studies. Second, salivary assays were used to estimate the DHEA hormone measures for this study, which are well-suited to developmental studies due to the non-invasive methodology. However, these samples are dependent on several factors (Herting and Sowell, 2017; Matchock et al., 2007) and are less sensitive to low hormone concentrations compared to other methods of hormone collection, which may be an issue at the onset of adrenarche (Herting and Sowell, 2017). Future studies should prospectively investigate participants to ensure that a more complete understanding of the adrenarcheal process is being captured. In fact, future work focusing on

how adrenarche impacts developing cortical dynamics may benefit from focusing on younger ages to assess changes specific to the onset of adrenarche. Additionally, the sulfated form of DHEA (DHEA-S) is thought to contribute to brain development, thus future studies could benefit from collecting both DHEA and DHEA-S. These studies should also consider using hair samples, which are more stable, to obtain more representative assays of hormone levels (Short et al., 2016). Together, more robust pubertal and hormonal assessments will allow for a greater understanding of how specific hormonal events relate to cortical dynamics during pubertal development.

## 5. Conclusion

Our study revealed that spontaneous cortical activity during childhood and adolescence is coupled with DHEA production and the interaction between DHEA and sex. Using MEG we found that delta power varied as a function of sex in the frontal and temporal cortices such that delta increased with DHEA in males, while females exhibited decreased delta with increasing DHEA. Sex-invariant DHEA effects were also seen, such that delta, beta and gamma increased in posterior cortices with increasing DHEA. Conversely, alpha exhibited decreased power with increasing DHEA. Our findings suggest that, above and beyond the influences of age, DHEA production is associated with changes in spontaneous cortical activity. Consistent with past work showing structural and oscillatory changes within the brain, these data provide further evidence for adrenal hormone development supporting neural dynamics during adolescent development. Future studies should probe the ties between DHEA and oscillatory activity serving task performance to further expand our understanding of adrenarche, as it relates to brain function. In summary, this novel study sheds light on the correspondence between DHEA and spontaneous cortical activity, above and beyond age, during the transition from childhood to adolescence. By understanding these relationships, we are making strides towards greater understanding of the contribution of adrenarche to neuronal development.

## Declaration of Competing Interest

The authors declare that they have no known competing financial interests or personal relationships that could have appeared to influence

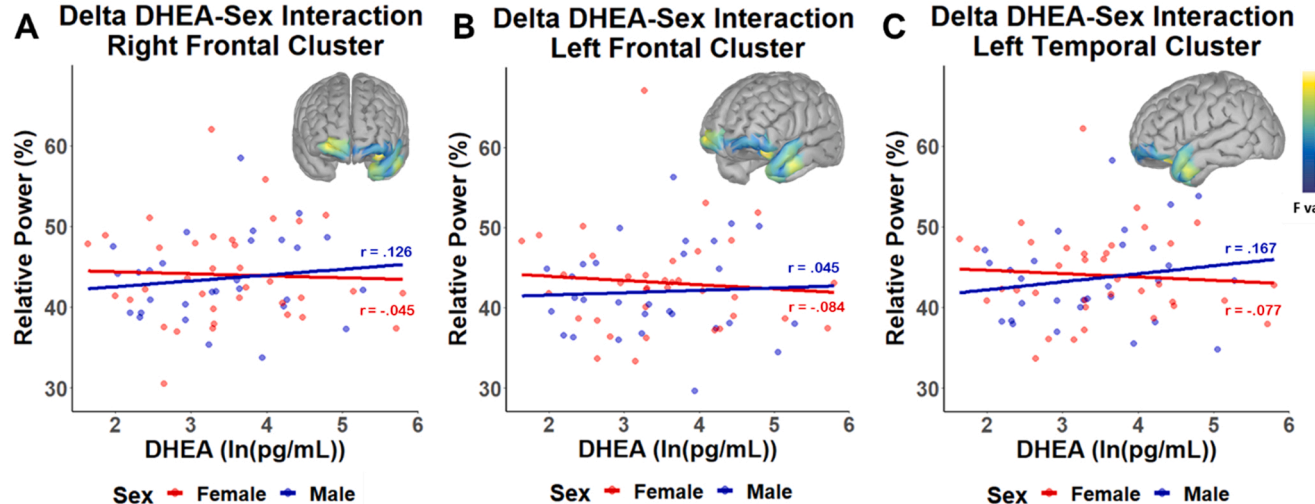


**Fig. 4.** Interaction Effect of DHEA and Sex: Scatter plots display the significant interaction between DHEA and sex in the delta frequency band. Relative delta power averaged across the cluster is plotted on the y-axis and natural log of DHEA on the x-axis in three separate clusters in the right frontal (A;  $r(\text{males}) = .126$ ,  $r(\text{females}) = .045$ ), left frontal (B;  $r(\text{males}) = .045$ ,  $r(\text{females}) = .084$ ) and left temporal (C;  $r(\text{males}) = .167$ ,  $r(\text{females}) = .077$ ) cortices. The blue circles and trendline on each plot represent males, while the green circles and trendline represent females. In all clusters, relative delta power increased with DHEA levels in males and decreased with DHEA levels in females. Thresholded TFCE maps are displayed with a color bar on the far right showing the scale of logged TFCE values.

the work reported in this paper.

## Data availability

The data used in this article will be made publicly available through the COINS framework at the completion of the study (<https://coins.trendscenter.org/>).

## Acknowledgements and Funding

This work was supported by the National Science Foundation of the USA (#1539067 and #2112455) and the National Institutes of Health (R01-MH121101, R01-MH116782, and P20-GM144641). The funders had no role in study design, data collection and analysis, decision to publish, or preparation of the manuscript. We would like to thank the participants for volunteering to participate in the study, as well as our staff and local collaborators for their contributions to the work. We would also like to specifically thank Nichole Knott for extensive help with the MEG recordings.

## References

Ashburner, J., Friston, K.J., 2005. Unified segmentation. *NeuroImage* 26 (3), 839–851. <https://doi.org/10.1016/j.neuroimage.2005.02.018>.

Baillet, S., Mosher, J.C., Leahy, R.M., 2001. Electromagnetic brain mapping. *IEEE Signal Process. Mag.* 18 (6), 14–30. <https://doi.org/10.1109/79.962275>.

Barendse, M.E.A., Simmons, J.G., Byrne, M.L., Seal, M.L., Patton, G., Mundy, L., Wood, S. J., Olsson, C.A., Allen, N.B., Whittle, S., 2018. Brain structural connectivity during adrenarche: associations between hormone levels and white matter microstructure. *Psychoneuroendocrinology* 88, 70–77. <https://doi.org/10.1016/j.psyneu.2017.11.009>.

Blakemore, S.-J., Burnett, S., Dahl, R.E., 2010. The role of puberty in the developing adolescent brain. *Hum. Brain Mapp.* 31 (6), 926–933. <https://doi.org/10.1002/hbm.21052>.

Bludau, S., Eickhoff, S.B., Mohlberg, H., Caspers, S., Laird, A.R., Fox, P.T., Schleicher, A., Zilles, K., Amunts, K., 2014. Cytoarchitecture, probability maps and functions of the human frontal pole. *NeuroImage* 93, 260–275. <https://doi.org/10.1016/j.neuroimage.2013.05.052>.

Buck Louis, G.M., Gray, L.E., Marcus, M., Ojeda, S.R., Pescovitz, O.H., Witchel, S.F., Sippell, W., Abbott, D.H., Soto, A., Tyl, R.W., Bourguignon, J.-P., Skakkebaek, N.E., Swan, S.H., Golub, M.S., Wabitsch, M., Toppari, J., Euling, S.Y., 2008. Environmental factors and puberty timing: expert panel research needs. *Pediatrics* 121 (Suppl 3), S192–S207. <https://doi.org/10.1542/peds.1813E>.

Byrne, M.L., Whittle, S., Vijayakumar, N., Dennison, M., Simmons, J.G., Allen, N.B., 2017. A systematic review of adrenarche as a sensitive period in neurobiological development and mental health. *Dev. Cogn. Neurosci.* 25, 12–28. <https://doi.org/10.1016/j.dcn.2016.12.004>.

Campbell, B., 2006. Adrenarche and the evolution of human life history. *Am. J. Hum. Biol.* 18 (5), 569–589. <https://doi.org/10.1002/ajhb.20528>.

Corpechot, C., Robel, P., Axelson, M., Sjövall, J., & Baulieu, E.E. (1981). Characterization and measurement of dehydroepiandrosterone sulfate in rat brain. *Proceedings of the National Academy of Sciences*, 78(8), 4704–4707. <https://doi.org/10.1073/pnas.78.8.4704>.

Dahl, R.E., 2004. Adolescent brain development: a period of vulnerabilities and opportunities. Keynote address. *Ann. N. Y. Acad. Sci.* 1021, 1–22. <https://doi.org/10.1196/annals.1308.001>.

Dale, A.M., Liu, A.K., Fischl, B.R., Buckner, R.L., Belliveau, J.W., Lewine, J.D., Halgren, E., 2000. Dyn. Stat. Parametr. Mapp.: Comb. fMRI MEG High. -Resolut. Imaging cortical Act. *Neuron* 26 (1), 55–67. [https://doi.org/10.1016/s0896-6273\(00\)81138-1](https://doi.org/10.1016/s0896-6273(00)81138-1).

Dorn, L.D., Chrousos, G.P., 1997. The neurobiology of stress: understanding regulation of affect during female biological transitions. *Semin. Reprod. Endocrinol.* 15 (1), 19–35. <https://doi.org/10.1055/s-2008-1067965>.

Embry, C.M., Wiesman, A.I., Proskovec, A.L., Mills, M.S., Heinrichs-Graham, E., Wang, Y.-P., Calhoun, V.D., Stephen, J.M., Wilson, T.W., 2019. Neural dynamics of verbal working memory processing in children and adolescents. *NeuroImage* 185, 191–197.

Fair, D.A., Cohen, A.L., Power, J.D., Dosenbach, N.U.F., Church, J.A., Miezin, F.M., Schlaggar, B.L., Petersen, S.E., 2009. Functional brain networks develop from a “local to distributed” organization. *PLoS Comput. Biol.* 5 (5), e1000381. <https://doi.org/10.1371/journal.pcbi.1000381>.

Fareri, D.S., Gabard-Durnam, L., Goff, B., Flannery, J., Gee, D.G., Lumian, D.S., Caldera, C., Tottenham, N., 2015. Normative development of ventral striatal resting state connectivity in humans. *NeuroImage* 118, 422–437. <https://doi.org/10.1016/j.neuroimage.2015.06.022>.

Fonov, V., Evans, A., McKinstry, R., Almlí, C.R., Collins, L., 2009. Unbiased nonlinear average age-appropriate brain templates from birth to adulthood. *NeuroImage* 47, [https://doi.org/10.1016/S1053-8119\(09\)70884-5](https://doi.org/10.1016/S1053-8119(09)70884-5).

Fung, M.H., Taylor, B.K., Frenzel, M.R., Eastman, J.A., Wang, Y.-P., Calhoun, V.D., Stephen, J.M., Wilson, T.W., 2020. Pubertal testosterone tracks the developmental trajectory of neural oscillatory activity serving visuospatial processing. *Cereb. Cortex* 30 (11), 5960–5971. <https://doi.org/10.1093/cercor/bhaa169>.

Fung, M.H., Taylor, B.K., Lew, B.J., Frenzel, M.R., Eastman, J.A., Wang, Y.-P., Calhoun, V.D., Stephen, J.M., Wilson, T.W., 2021. Sexually dimorphic development in the cortical oscillatory dynamics serving early visual processing. *Dev. Cogn. Neurosci.* 50, 100968. <https://doi.org/10.1016/j.dcn.2021.100968>.

Fuster, J.M., 2002. Frontal lobe and cognitive development. *J. Neurocytol.* 31 (3), 373–385. <https://doi.org/10.1023/A:1024190429920>.

Goddings, A.-L., Burnett Heyes, S., Bird, G., Viner, R.M., Blakemore, S.-J., 2012. The relationship between puberty and social emotion processing. *Dev. Sci.* 15 (6), 801–811. <https://doi.org/10.1111/j.1467-7687.2012.01174.x>.

Goddings, A.-L., Beltz, A., Peper, J.S., Crone, E.A., Braams, B.R., 2019. Understanding the role of puberty in structural and functional development of the adolescent brain. *J. Res. Adolesc.* 29 (1), 32–53. <https://doi.org/10.1111/jora.12408>.

Gaser, C., Dahnke, R., Thompson, P., Kurth, F., Luders, E., Alzheimer's Disease Neuroimaging Initiative., (2022). CAT - A Computational Anatomy Toolbox for the Analysis of Structural MRI Data. *bioRxiv* 2022.06.11.495736; doi: <https://doi.org/10.1101/2022.06.11.495736>.

Gogtay, N., Giedd, J.N., Lusk, L., Hayashi, K.M., Greenstein, D., Vaituzis, A.C., Nugent, T. F., Herman, D.H., Clasen, L.S., Toga, A.W., Rapoport, J.L., & Thompson, P.M. (2004). Dynamic mapping of human cortical development during childhood through early adulthood. *Proceedings of the National Academy of Sciences of the United States of America*, 101(21), 8174–8179. <https://doi.org/10.1073/pnas.0402680101>.

Gómez, C., Pérez-Macías, J.M., Poza, J., Fernández, A., Hornero, R., 2013. Spectral changes in spontaneous MEG activity across the lifespan. *J. Neural Eng.* 10 (6), 066006. <https://doi.org/10.1088/1741-2560/10/6/066006>.

Harden, K.P., Kretsch, N., Tackett, J.L., Tucker-Drob, E.M., 2014. Genetic and environmental influences on testosterone in adolescents: evidence for sex differences. *Dev. Psychobiol.* 56 (6), 1278–1289.

Heinrichs-Graham, E., Wilson, T.W., 2015. Spatiotemporal oscillatory dynamics during the encoding and maintenance phases of a visual working memory task. *Cortex; a J. Devoted Study Nerv. Syst. Behav.* 69, 121–130. <https://doi.org/10.1016/j.cortex.2015.04.022>.

Heinrichs-Graham, E., McDermott, T.J., Mills, M.S., Wiesman, A.I., Wang, Y.-P., Stephen, J.M., Calhoun, V.D., Wilson, T.W., 2018. The lifespan trajectory of neural oscillatory activity in the motor system. *Dev. Cogn. Neurosci.* 30, 159–168.

Herting, M.M., Sowell, E.R., 2017. Puberty and structural brain development in humans. *Front. Neuroendocrinol.* 44, 122–137. <https://doi.org/10.1016/j.yfrne.2016.12.003>.

Huang, M.X., Mosher, J.C., Leahy, R.M., 1999. A sensor-weighted overlapping-sphere head model and exhaustive head model comparison for MEG. *Phys. Med. Biol.* 44 (2), 423–440. <https://doi.org/10.1088/0031-9155/44/2/010>.

Ille, N., Berg, P., Scherg, M., 2002. Artifact correction of the ongoing EEG using spatial filters based on artifact and brain signal topographies. *J. Clin. Neurophysiol. Off. Publ. Am. Electroencephalogr. Soc.* 19 (2), 113–124. <https://doi.org/10.1097/00004691-200203000-00002>.

Killanin, A.D., Wiesman, A.I., Heinrichs-Graham, E., Groff, B.R., Frenzel, M.R., Eastman, J.A., Wang, Y.-P., Calhoun, V.D., Stephen, J.M., Wilson, T.W., 2020. Development and sex modulate visuospatial oscillatory dynamics in typically-developing children and adolescents. *NeuroImage* 221 (117192). <https://doi.org/10.1016/j.neuroimage.2020.117192>.

Killanin, A.D., Embury, C.M., Picci, G., Heinrichs-Graham, E., Wang, Y.-P., Calhoun, V. D., Stephen, J.M., Wilson, T.W., 2022. Trauma moderates the development of the oscillatory dynamics serving working memory in a sex-specific manner. *Cereb. Cortex*.

Klapwijk, E.T., Goddings, A.-L., Heyes, S.B., Bird, G., Viner, R.M., Blakemore, S.-J., 2013. Increased functional connectivity with puberty in the mentalising network involved in social emotion processing. *Horm. Behav.* 64 (2), 314–322. <https://doi.org/10.1016/j.yhbeh.2013.03.012>.

Klauser, P., Whittle, S., Simmons, J.G., Byrne, M.L., Mundy, L.K., Patton, G.C., Fornito, A., Allen, N.B., 2015. Reduced frontal white matter volume in children with early onset of adrenarche. *Psychoneuroendocrinology* 52, 111–118. <https://doi.org/10.1016/j.psyneu.2014.10.020>.

Manjón, J.V., Coupé, P., Martí-Bonmatí, L., Collins, D.L., Robles, M., 2010. Adaptive non-local means denoising of MR images with spatially varying noise levels. *J. Magn. Reson. Imaging* 31 (1), 192–203. <https://doi.org/10.1002/jmri.22003>.

Matchock, R.L., Dorn, L.D., Susman, E.J., 2007. Diurnal and seasonal cortisol, testosterone, and DHEA rhythms in boys and girls during puberty. *Chronobiol. Int.* 24 (5), 969–990. <https://doi.org/10.1080/07420520701649471>.

McDermott, T.J., Wiesman, A.I., Proskovec, A.L., Heinrichs-Graham, E., Wilson, T.W., 2017. Spatiotemporal oscillatory dynamics of visual selective attention during a flanker task. *NeuroImage* 156, 277–285. <https://doi.org/10.1016/j.neuroimage.2017.05.014>.

Mellon, S.H., Griffin, L.D., 2002. Neurosteroids: biochemistry and clinical significance. *Trends Endocrinol. Metab.* 13 (1), 35–43.

Misselhorn, J., Fries, U., Engel, A.K., 2019. Frontal and parietal alpha oscillations reflect attentional modulation of cross-modal matching. *Sci. Rep.* 9 (1), 5030. <https://doi.org/10.1038/s41598-019-41636-w>.

Morandini, H.A.E., Rao, P., Hood, S.D., Zepf, F.D., Silk, T.J., Griffiths, K.R., 2021. Age-related resting-state functional connectivity of the Vigilant Attention network in children and adolescents. *Brain Cogn.* 154, 105791. <https://doi.org/10.1016/j.bandc.2021.105791>.

Murray, C.R., Simmons, J.G., Allen, N.B., Byrne, M.L., Mundy, L.K., Seal, M.L., Patton, G. C., Olsson, C.A., Whittle, S., 2016. Associations between dehydroepiandrosterone

(DHEA) levels, pituitary volume, and social anxiety in children. *Psychoneuroendocrinology* 64, 31–39. <https://doi.org/10.1016/j.psyneuen.2015.11.004>.

Nguyen, T.-V., McCracken, J.T., Ducharme, S., Cropp, B.F., Botteron, K.N., Evans, A.C., Karama, S., 2013. Interactive effects of dehydroepiandrosterone and testosterone on cortical thickness during early brain development. *J. Neurosci.* 33 (26), 10840–10848. <https://doi.org/10.1523/JNEUROSCI.5747-12.2013>.

Nguyen, T.-V., Gower, P., Albaugh, M.D., Botteron, K.N., Hudziak, J.J., Fonov, V.S., Collins, L., Ducharme, S., McCracken, J.T., 2016. The developmental relationship between DHEA and visual attention is mediated by structural plasticity of corticoamygdalar networks. *Psychoneuroendocrinology* 70, 122–133. <https://doi.org/10.1016/j.psyneuen.2016.05.003>.

Niso, G., Tadel, F., Bock, E., Cousineau, M., Santos, A., Baillet, S., 2019. Brainstorm pipeline analysis of resting-state data from the open MEG archive. *Front. Neurosci.* 13. <https://doi.org/10.3389/fnins.2019.00284>.

Orentreich, N., Brind, J.L., Rizer, R.L., Vogelman, J.H., 1984. Age changes and sex differences in serum dehydroepiandrosterone sulfate concentrations throughout adulthood. *J. Clin. Endocrinol. Metab.* 59 (3), 551–555. <https://doi.org/10.1210/jcem-59-3-551>.

Ott, L.R., Penhale, S.H., Taylor, B.K., Lew, B.J., Wang, Y.-P., Calhoun, V.D., Stephen, J.M., Wilson, T.W., 2021. Spontaneous cortical MEG activity undergoes unique age- and sex-related changes during the transition to adolescence. *NeuroImage* 244, 118552. <https://doi.org/10.1016/j.neuroimage.2021.118552>.

Proskovec, A.L., Heinrichs-Graham, E., Wilson, T.W., 2016. Aging modulates the oscillatory dynamics underlying successful working memory encoding and maintenance. *Hum. Brain Mapp.* 37 (6), 2348–2361. <https://doi.org/10.1002/hbm.23178>.

Proskovec, A.L., Heinrichs-Graham, E., Wiesman, A.I., McDermott, T.J., Wilson, T.W., 2018. Oscillatory dynamics in the dorsal and ventral attention networks during the reorienting of attention. *Hum. Brain Mapp.* 39 (5), 2177–2190. <https://doi.org/10.1002/hbm.23997>.

Prough, R.A., Clark, B.J., Klinge, C.M., 2016. Novel mechanisms for DHEA action. *J. Mol. Endocrinol.* 56 (3), R139–R155. <https://doi.org/10.1530/JME-16-0013>.

Racchi, M., Baldazzi, C., Corsini, E., 2003. Dehydroepiandrosterone (DHEA) and the aging brain: flipping a coin in the “fountain of youth”. *CNS Drug Rev.* 9 (1), 21–40. <https://doi.org/10.1111/j.1527-3458.2003.tb00242.x>.

Rainey, W.E., Carr, B.R., Sasano, H., Suzuki, T., Mason, J.I., 2002. Dissecting human adrenal androgen production. *Trends Endocrinol. Metab.* TEM 13 (6), 234–239. [https://doi.org/10.1016/s1043-2760\(02\)00609-4](https://doi.org/10.1016/s1043-2760(02)00609-4).

Rajapakse, J.C., Giedd, J.N., Rapoport, J.L., 1997. Statistical approach to segmentation of single-channel cerebral MR images. *IEEE Trans. Med. Imaging* 16 (2), 176–186. <https://doi.org/10.1109/42.563663>.

Romine, C.B., Reynolds, C.R., 2005. A model of the development of frontal lobe functioning: findings from a meta-analysis. *Appl. Neuropsychol.* 12 (4), 190–201. [https://doi.org/10.1207/s15324826an1204\\_2](https://doi.org/10.1207/s15324826an1204_2).

Shaw, P., Kabani, N.J., Lerch, J.P., Eckstrand, K., Lenroot, R., Gogtay, N., Greenstein, D., Clasen, L., Evans, A., Rapoport, J.L., Giedd, J.N., Wise, S.P., 2008. Neurodevelopmental trajectories of the human cerebral cortex. *J. Neurosci.: Off. J. Soc. Neurosci.* 28 (14), 3586–3594. <https://doi.org/10.1523/JNEUROSCI.5309-07.2008>.

Short, S.J., Stalder, T., Marceau, K., Entringer, S., Moog, N.K., Shirtcliff, E.A., Wadhwa, P.D., Buss, C., 2016. Correspondence between hair cortisol concentrations and 30-day integrated daily salivary and weekly urinary cortisol measures. *Psychoneuroendocrinology* 71, 12–18. <https://doi.org/10.1016/j.psyneuen.2016.05.007>.

Smith, S.M., Nichols, T.E., 2009. Threshold-free cluster enhancement: addressing problems of smoothing, threshold dependence and localisation in cluster inference. *NeuroImage* 44 (1), 83–98. <https://doi.org/10.1016/j.neuroimage.2008.03.061>.

Sowell, E.R., Thompson, P.M., Leonard, C.M., Welcome, S.E., Kan, E., Toga, A.W., 2004. Longitudinal mapping of cortical thickness and brain growth in normal children. *J. Neurosci.: Off. J. Soc. Neurosci.* 24 (38), 8223–8231. <https://doi.org/10.1523/JNEUROSCI.1798-04.2004>.

Sripada, R.K., Welsh, R.C., Marx, C.E., Liberzon, I., 2013. The neurosteroids allopregnanolone and dehydroepiandrosterone modulate resting-state amygdala connectivity. *Hum. Brain Mapp.* 35 (7), 3249–3261. <https://doi.org/10.1002/hbm.22399>.

Sulková, J., Hill, M., Hampl, R., Stárka, L., 1997. Age and sex related differences in serum levels of unconjugated dehydroepiandrosterone and its sulphate in normal subjects. *J. Endocrinol.* 154 (1), 57–62. <https://doi.org/10.1677/joe.0.1540057>.

Tadel, F., Bock, E., Niso, G., Mosher, J.C., Cousineau, M., Pantazis, D., Leahy, R.M., Baillet, S., 2019. MEG/EEG group analysis with brainstorm. *Front. Neurosci.* 13. <https://doi.org/10.3389/fnins.2019.00076>.

Taulu, S., Simola, J., 2006. Spatiotemporal signal space separation method for rejecting nearby interference in MEG measurements. *Phys. Med. Biol.* 51 (7), 1759–1768. <https://doi.org/10.1088/0031-9155/51/7/008>.

Taylor, B.K., Embury, C.M., Heinrichs-Graham, E., Frenzel, M.R., Eastman, J.A., Wiesman, A.I., Wang, Y.-P., Calhoun, V.D., Stephen, J.M., Wilson, T.W., 2020. Neural oscillatory dynamics serving abstract reasoning reveal robust sex differences in typically-developing children and adolescents. *Dev. Cogn. Neurosci.* 42, 100770. <https://doi.org/10.1016/j.dcn.2020.100770>.

Taylor, B.K., Eastman, J.A., Frenzel, M.R., Embury, C.M., Wang, Y.-P., Calhoun, V.D., Stephen, J.M., Wilson, T.W., 2021. Neural oscillations underlying selective attention follow sexually divergent developmental trajectories during adolescence. *Dev. Cogn. Neurosci.* 49, 100961. <https://doi.org/10.1016/j.dcn.2021.100961>.

Tohka, J., Zijdenbos, A., Evans, A., 2004. Fast and robust parameter estimation for statistical partial volume models in brain MRI. *NeuroImage* 23 (1), 84–97. <https://doi.org/10.1016/j.neuroimage.2004.05.007>.

Trevarrow, M.P., Kurz, M.J., McDermott, T.J., Wiesman, A.I., Mills, M.S., Wang, Y.-P., Calhoun, V.D., Stephen, J.M., Wilson, T.W., 2019. The developmental trajectory of sensorimotor cortical oscillations. *NeuroImage* 184, 455–461.

Tsujimoto, S., Genovesio, A., Wise, S.P., 2011. Frontal pole cortex: encoding ends at the end of the endbrain. *Trends Cogn. Sci.* 15 (4), 169–176. <https://doi.org/10.1016/j.tics.2011.02.001>.

Uusitalo, M., Ilmoniemi, R., 1997. Signal-space projection method for separating MEG or EEG into components. *Med. Biol. Eng. Comput.* 35, 135–140. <https://doi.org/10.1007/BF02534144>.

Vlahou, E.L., Thurm, F., Kolassa, I.-T., Schlee, W., 2014. Resting-state slow wave power, healthy aging and cognitive performance. *Sci. Rep.* 4 (1), 5101. <https://doi.org/10.1038/srep05101>.

Wang, J., Barstein, J., Ethridge, L.E., Mosconi, M.W., Takarae, Y., Sweeney, J.A., 2013. Resting state EEG abnormalities in autism spectrum disorders. *J. Neurodev. Disord.* 5 (1), 24. <https://doi.org/10.1186/1866-1955-5-24>.

Welch, P., 1967. The use of fast Fourier transform for the estimation of power spectra: a method based on time averaging over short, modified periodograms. *IEEE Trans. Audio Electro* 15 (2), 70–73. <https://doi.org/10.1109/TAU.1967.1161901>.

Whittle, S., Simmons, J.G., Byrne, M.L., Strikwerda-Brown, C., Kerestes, R., Seal, M.L., Olsson, C.A., Dudgeon, P., Mundy, L.K., Patton, G.C., Allen, N.B., 2015. Associations between early adrenarche, affective brain function and mental health in children. *Soc. Cogn. Affect. Neurosci.* 10 (9), 1282–1290. <https://doi.org/10.1093/scan/nsv014>.

Whittle, S., Barendse, M., Pozzi, E., Vijayakumar, N., Simmons, J.G., 2020. Pubertal hormones predict sex-specific trajectories of pituitary gland volume during the transition from childhood to adolescence. *NeuroImage* 204, 116256. <https://doi.org/10.1016/j.neuroimage.2019.116256>.

Wierenga, L.M., Langen, M., Oranje, B., Durston, S., 2014. Unique developmental trajectories of cortical thickness and surface area. *NeuroImage* 87, 120–126. <https://doi.org/10.1016/j.neuroimage.2013.11.010>.

Wierenga, L.M., Bos, M.G.N., Schreuders, E., vd Kamp, F., Peper, J.S., Tamnes, C.K., Crone, E.A., 2018. Unraveling age, puberty and testosterone effects on subcortical brain development across adolescence. *Psychoneuroendocrinology* 91, 105–114. <https://doi.org/10.1016/j.psyneuen.2018.02.034>.

Wiesman, A.I., Heinrichs-Graham, E., Proskovec, A.L., McDermott, T.J., Wilson, T.W., 2017. Oscillations during observations: dynamic oscillatory networks serving visuospatial attention. *Hum. Brain Mapp.* 38 (10), 5128–5140. <https://doi.org/10.1002/hbm.23720>.

Wilson, T.W., Slason, E., Asherin, R., Kronberg, E., Reite, M.L., Teale, P.D., Rojas, D.C., 2010. An extended motor network generates beta and gamma oscillatory perturbations during development. *Brain Cogn.* 73 (2), 75–84. <https://doi.org/10.1016/j.bandc.2010.03.001>.

Wilson, T.W., Proskovec, A.L., Heinrichs-Graham, E., O'Neill, J., Robertson, K.R., Fox, H.S., Swindells, S., 2017. Aberrant neuronal dynamics during working memory operations in the aging HIV-infected brain. *Sci. Rep.* 7, 41568. <https://doi.org/10.1038/srep41568>.

Zaretskaya, N., Bartels, A., 2015. Gestalt perception is associated with reduced parietal beta oscillations. *NeuroImage* 112, 61–69. <https://doi.org/10.1016/j.neuroimage.2015.02.049>.